

## **DECK CONTRACTION INDUCED DEFLECTION IN A HIGH PERFORMANCE CONCRETE BRIDGE**

**Marvin L. Griffin, PE**, Dept. of Civil and Mechanical Engineering, United States Military Academy, West Point, NY

**Lawrence F. Kahn, PhD, PE**, School of Civil and Environmental Engineering, Georgia Institute of Technology, Atlanta, GA

**Mauricio Lopez**, School of Civil and Environmental Engineering, Georgia Institute of Technology, Atlanta, GA

### **ABSTRACT**

*This paper examines deflections in a high performance concrete bridge. Experimental data revealed 0.54 inches of excess downward displacement after the application of the dead load and beyond standard design predictions. A finite element model replicated and confirmed the results of the bridge measurements. Experimental data and analytical results suggest that contraction of the bridge deck was the primary cause of the additional displacement. The authors provide a simplified method for predicting deflections induced by deck contraction.*

**Keywords:** Bridge, High-Performance Concrete, Deflection, Temperature, Shrinkage, Deck Contraction

### **INTRODUCTION**

The purpose of this study was to investigate the deflections of a high performance concrete (HPC) highway bridge due to shrinkage and temperature changes in the deck and to compare those deflections to analytical predictions. As part of on-going research sponsored by the Georgia Department of Transportation and the Federal Highway Administration, an HPC bridge in Georgia was evaluated in order to determine the impacts of deck shrinkage and temperature changes. The bridge was a four-span structure using precast prestressed girders with a composite deck over Interstate 75 in Henry County, Georgia, approximately 15 miles southeast of Atlanta, Georgia (Figure 1). The bridge was constructed in two phases, with each phase supporting 3 lanes of the 6 lane bridge. The evaluation of deck shrinkage and temperature changes was limited to Phase 2 of the Georgia HPC bridge project.

### **OVERVIEW OF THE PROJECT**

The 353 ft (107.6 m) long bridge was 94 ft (28.7 m) wide; Phases 1 and 2 each were 47 ft (14.3 m) wide. Each of the four spans was simply-supported with 13 HPC girders made

with design strengths of 10,280 psi (70 MPa) and center-to-center bearing lengths specified in Table 1. Figures 2 and 3 depict the plan and elevation view of the bridge layout. Concrete diaphragms were used at midspan locations for spans 1 and 4, while spans 2 and 3 had diaphragms at 1/3 span lengths.



Figure 1. Span 2, Phase 1 of the Georgia HPC bridge.

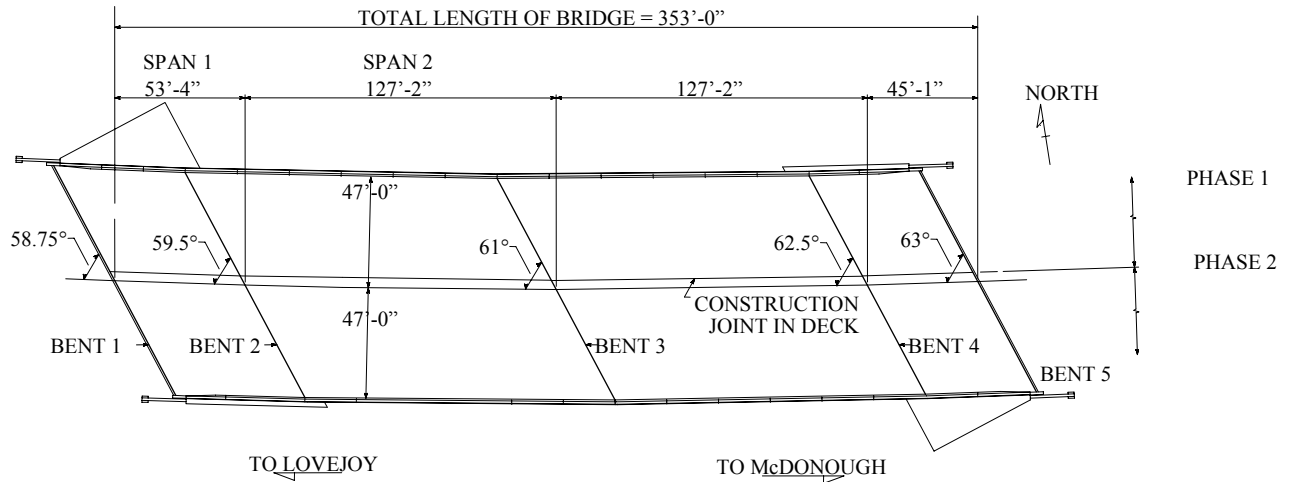


Figure 2. Bridge plan view.

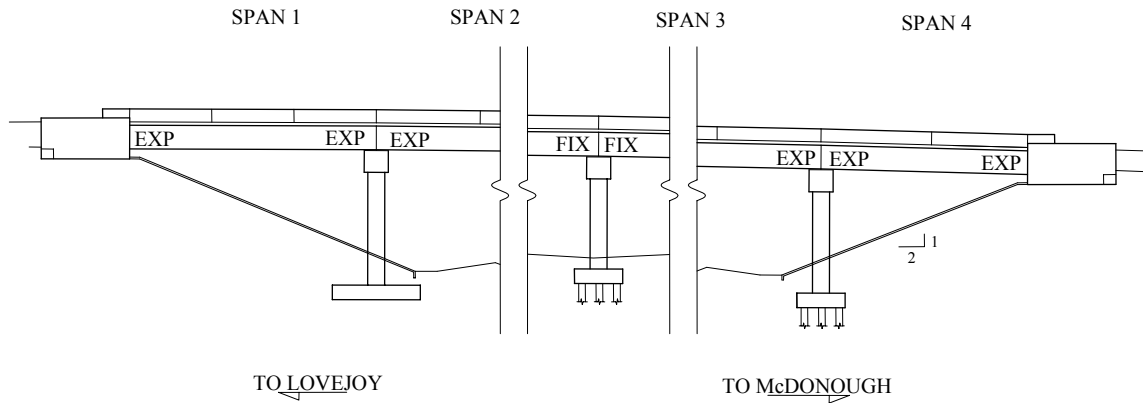


Figure 3. Bridge south elevation.

Table 1. Span length and specifications for Phase 2.

Span	Supported Length	AASHTO Type Girders	Number of Girders
1	50 ft 1 in (15.26 m)	II	6
		IV	1
2	124 ft 1 in (37.82 m)	IV	7
3	124 ft 1 in (37.82 m)	IV	7
4	42 ft 0 in (12.8 m)	II	6
		IV	1

The HPC bridge deck had a design strength of 7000 psi (48 MPa) and a maximum specified rapid chloride permeability at 56 days of 2000 coulombs. The deck was formed with galvanized steel deck forms which were connected to the girders with welded shear connectors. The mild steel reinforced concrete deck was approximately 8 inches (203 mm) thick above the top of the forms; the top reinforcing mat had a cover of 2.75 in (70 mm) and was epoxy coated while the bottom mat had a 1 in (25.4 mm) cover above the metal decking. Finally, a cast-in-place normal strength (3500 psi, 24 MPa) concrete barrier was constructed on each side of the bridge.

Slapkus and Kahn (2002) evaluated and tested the strength and elastic modulus for the bridge girders. The average results of their tests are outlined in Table 2 below. The coefficient of thermal expansion for the girders was determined experimentally by Shams

and Kahn (2000) for grade 2 high-performance concrete. Compressive strength, elastic modulus, and CTE tests were conducted on deck concrete from Phase 1 and Phase 2 of the project. CTE tests are summarized in Table 2 and discussed later.

Table 2. Mechanical properties of bridge deck and girders for Phase 2.

Component	Phase	56-day Compressive Strength (fc')	56-day Modulus of Elasticity (Ec)	56-day Coefficient of Thermal Expansion (CTE)
Deck	1	6,880 psi (47 MPa)	3,673 ksi (25.3 GPa)	6.35 $\mu\epsilon/^\circ\text{F}$ (11.43 mm/mm/ $^\circ\text{C}$ )
Deck	2	7,311 psi (50 MPa)	3,600 ksi (24.8 GPa)	4.95 $\mu\epsilon/^\circ\text{F}$ (8.91 mm/mm/ $^\circ\text{C}$ )
	Curing			
Type II Girders	ASTM	13,380 psi (92 MPa)	4,983 ksi (34.4 GPa)	5.13 $\mu\epsilon/^\circ\text{F}$ (9.23 mm/mm/ $^\circ\text{C}$ )
Type II	Match	12,800 psi (88 MPa)	5,031 ksi (34.7 GPa)	5.13 $\mu\epsilon/^\circ\text{F}$ (9.23 mm/mm/ $^\circ\text{C}$ )
Type IV	ASTM	13,160 psi (91 MPa)	4,962 ksi (34.2 GPa)	5.13 $\mu\epsilon/^\circ\text{F}$ (9.23 mm/mm/ $^\circ\text{C}$ )
Type IV	Match	12,050 psi (83 MPa)	4,911 ksi (33.9 GPa)	5.13 $\mu\epsilon/^\circ\text{F}$ (9.23 mm/mm/ $^\circ\text{C}$ )

One year after the construction of Phase 1, the researchers found larger deflections than predicted analytically. Slapkus and Kahn (2002) predicted that the total dead-load deflection would yield an upward camber of 0.71 inches (18 mm) in span 2 of the bridge. Measurements of the deflection, however, showed a downward displacement of 1.3 inches (33 mm). It was hypothesized that the excess deflection was due to shrinkage and/or temperature changes in the bridge deck. To better understand this long term deflection, span 2 of Phase 2 deck was instrumented for deflection, strain, and temperature measurements.

## INSTRUMENTATION

The Phase 2 deck was cast 14 months after the girders. When the deck was cast, the potential existed for the deck to bond to the girders and then shrink. This differential shrinkage could then lead to an overall downward deflection.

In order to identify a potential cause of the displacements, span 2, phase 2 of the project was instrumented and evaluated. Span 2, the focus of the investigation, included deflection measurements of three center girders, girders 2.9, 2.10, and 2.11 as shown in Figures 4 and 6. Deflections were measured at 40% of the span length (0.4 L), approximately 50 ft (15.2 m) from the center of the west bearing so that personnel could stand on the roadside shoulder beneath the span and monitor the deflection rods hung from the bottom flanges (Figures 4 and 5).

Strain gages were located within the concrete deck and at the top of the girders to measure and extract a strain profile for the composite section. Eight embedded electrical resistance strain gages were tied to the top and bottom deck reinforcing steel at locations A, B, and C as shown in Figure 6. Two additional electrical resistance strain gages were epoxy bonded to the top surface of girder 2.10 at midspan (location C). Two vibrating wire strain gages were also placed along the top and bottom deck reinforcement at the midspan (location C), directly above girders 2.9 and 2.10. Finally, six thermocouples were placed adjacent to strain gages at locations A and C to measure the heat of hydration in the deck and ambient temperature changes. Location A is at 1/8 of the span length, while locations B and C are at the quarter and midpoints of the span, respectively. Figures 7 and 8 depict the specific placement of each gage within the deck-girder composite section.

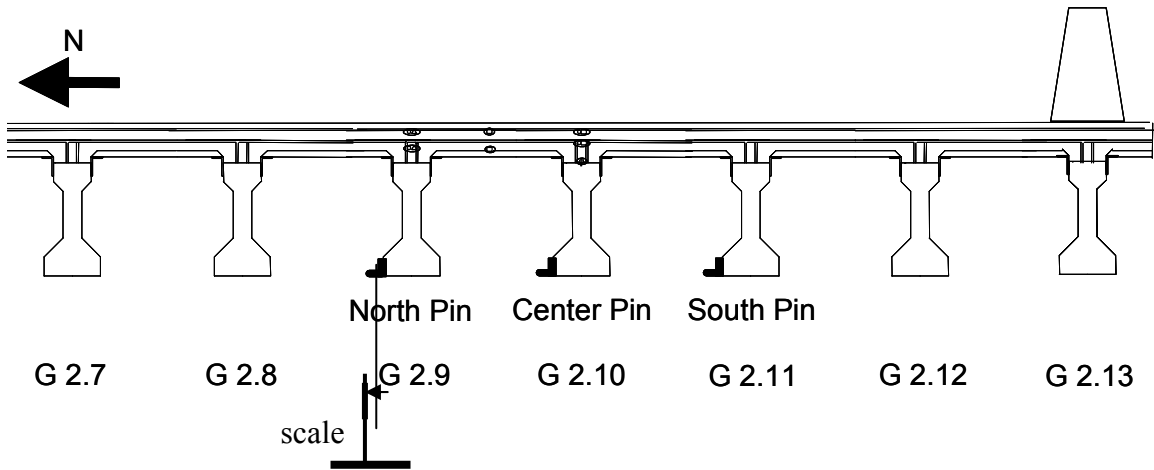


Figure 4. Deflection rods (40% L).



Figure 5. Photo of Deflection Rod Measurements.

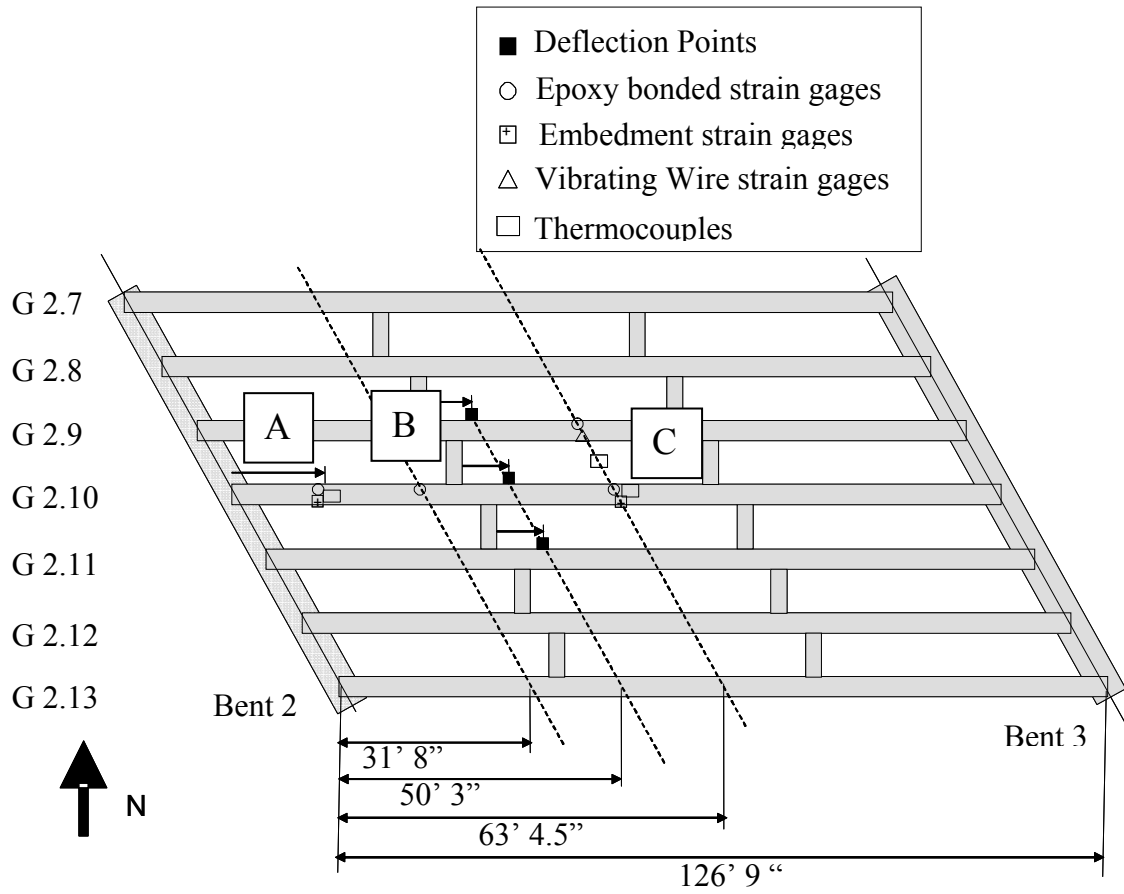


Figure 6. Instrumentation layout, span 2, Phase 2.

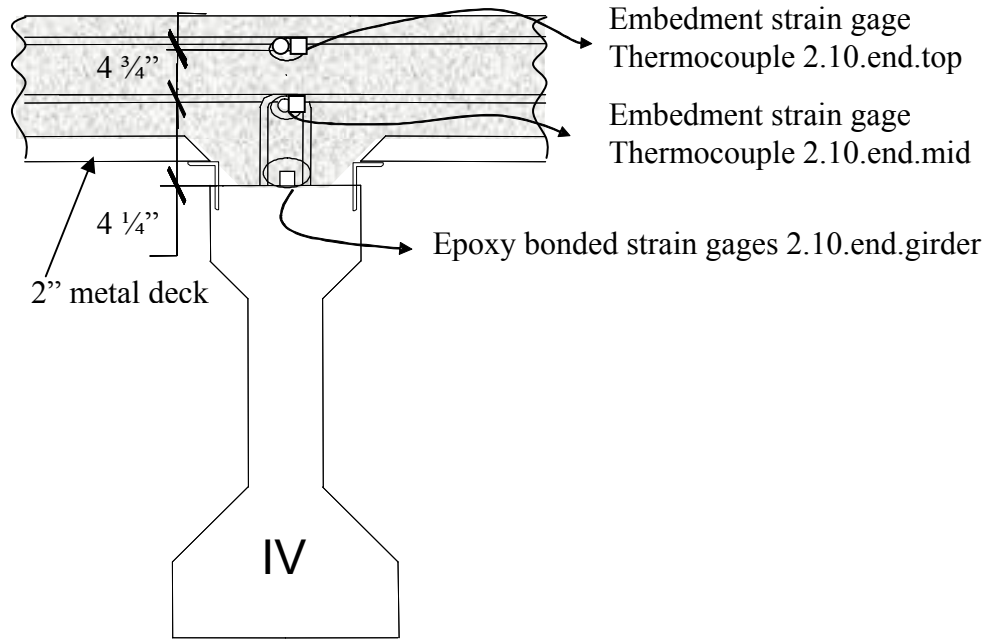


Figure 7. Instrumentation elevation location A (1/8 L).

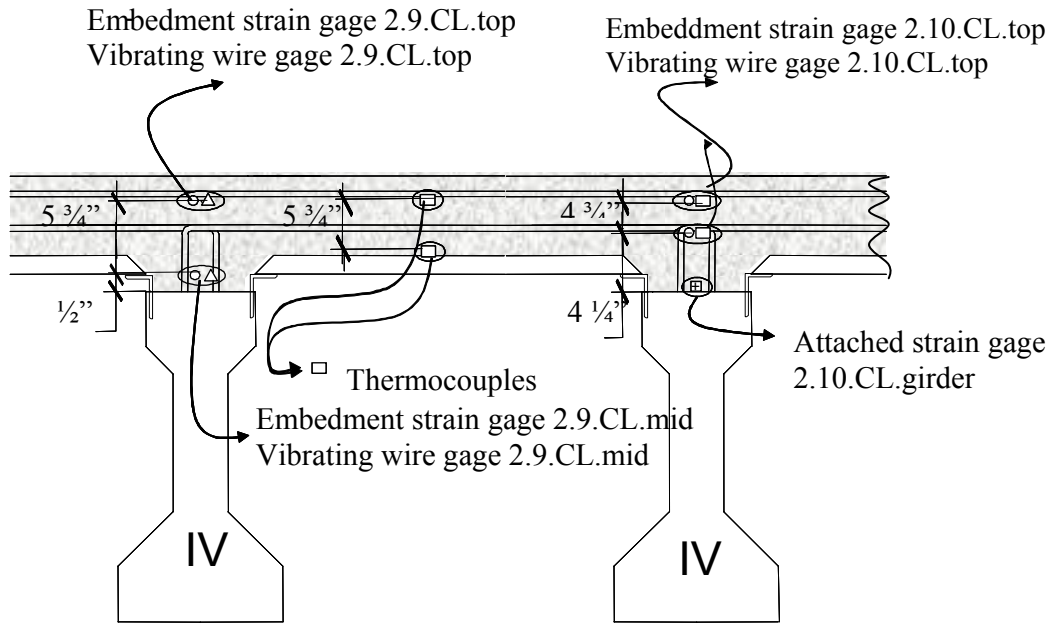


Figure 8. Instrumentation elevation location C (midspan).

## MATERIAL TESTING AND RESULTS

Four of the 13 trucks used to pour the Phase 2 deck were sampled for testing and quality control; 27 cylinder samples from each of the four trucks were used to determine

compressive strength and elastic modulus. Three 4 x 15 inch (102 x 381 mm) cylinder specimens were sampled in order to evaluate the coefficient of thermal expansion, and six 22 x 7 x 7 inch (558 x 178 mm) prismatic specimens were made for shrinkage testing.

The compressive strengths, determined using 6 x 12 in cylinders and tested at 56-days, ranged between 7,054 (49 MPa) to 7,693 psi (53 MPa), with an average of 7311 psi (50 MPa). Figure 9 shows the results of compression testing over time.

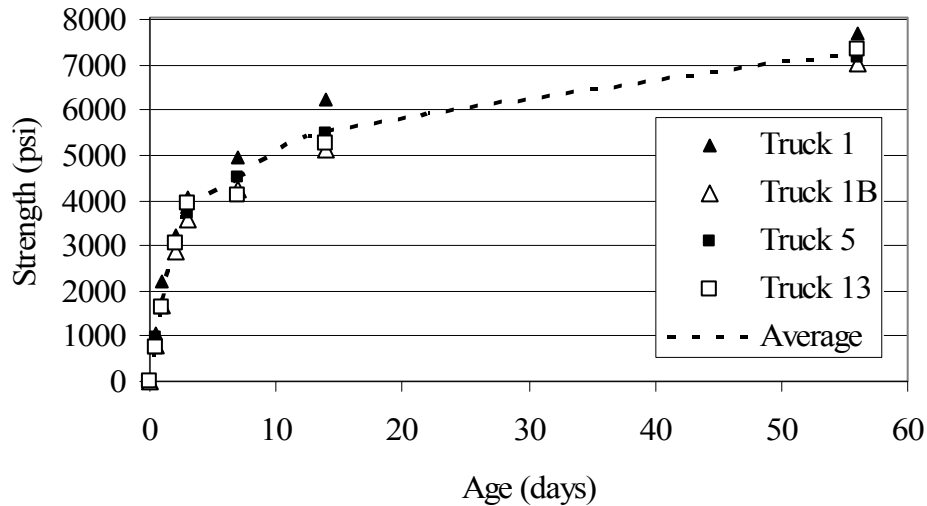


Figure 9. Compressive strength for deck concrete, Phase 2, span 2.

The 7, 14, and 90-day modulus of elasticity for the deck concrete was also tested in accordance with ASTM C 469. The 7-day elastic modulus ranged from 2,914 (20,092 MPa) to 3,326 ksi (22,932 MPa), with an average of 3,098 ksi (21,370 MPa). The 14-day elastic modulus ranged from 3,103 (21,395 MPa) to 3,454 ksi (23,815 MPa), with an average of 3,228 ksi (22,257 MPa). Finally, the 90-day elastic modulus ranged from 3,383 (23,325 MPa) to 3,753 ksi (25,877 MPa), with an average of 3,613 ksi (24,911 MPa). Figure 10 depicts the change in modulus over time.

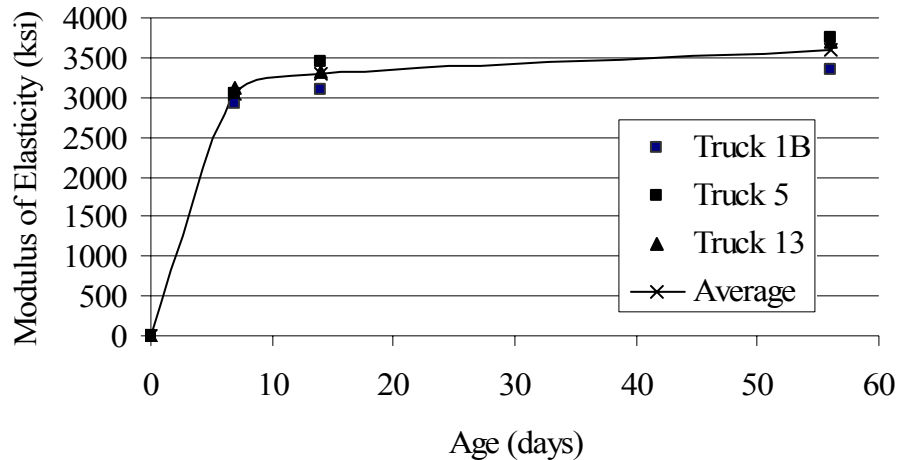


Figure 10. Deck modulus of elasticity, Phase 2, span 2.

The coefficient of thermal expansion was measured using 4 x 15 inch (102 x 381 mm) specimens at 6 and 70 days according to the Army Corps of Engineer's procedure (CRD-C39). The 4 x 15 inch (102 x 381 mm) cylinders were kept outside under ambient conditions (69 % average relative humidity) in order to match the conditions of the actual bridge. The CTE results were  $6.28 \mu\epsilon/^{\circ}\text{F}$  ( $11.3 \mu\epsilon/^{\circ}\text{C}$ ) at 6 days and  $3.66 \mu\epsilon/^{\circ}\text{F}$  ( $6.59 \mu\epsilon/^{\circ}\text{C}$ ) at 70 days. The decrease in the coefficient of thermal expansion reflects the change in water content over time.

Shrinkage of the deck concrete was measured using six 22 x 7 x 7 inch (558 x 178 mm) prismatic samples. Shrinkage measurements began 6 hours after casting with embedded variable-resistance strain gages. The axial strain gage results are presented in Figure 11. At 65 days after casting, the specimens contracted an average of 128 microstrains at the midplane. The majority of the strain occurred from 0 to 30 days after placement. The sample temperature at casting was  $64^{\circ}\text{F}$  ( $17.8^{\circ}\text{C}$ ), while the sample temperature at 30 days was  $34^{\circ}\text{F}$  ( $1^{\circ}\text{C}$ ). After day 30, the ambient temperature was nearly constant for the remainder of the tests. Using an average CTE of  $5.0 \mu\epsilon/^{\circ}\text{F}$  ( $9 \mu\epsilon/^{\circ}\text{C}$ ), a compressive strain of approximately  $150 \mu\epsilon$  would be expected for the  $30^{\circ}\text{F}$  ( $9^{\circ}\text{C}$ ) compressive temperature change; this value is slightly greater than the  $-130$  compressive strain in the shrinkage specimens. Therefore, the shrinkage strains were small or non-existent; the contraction strain was due to the temperature decrease.

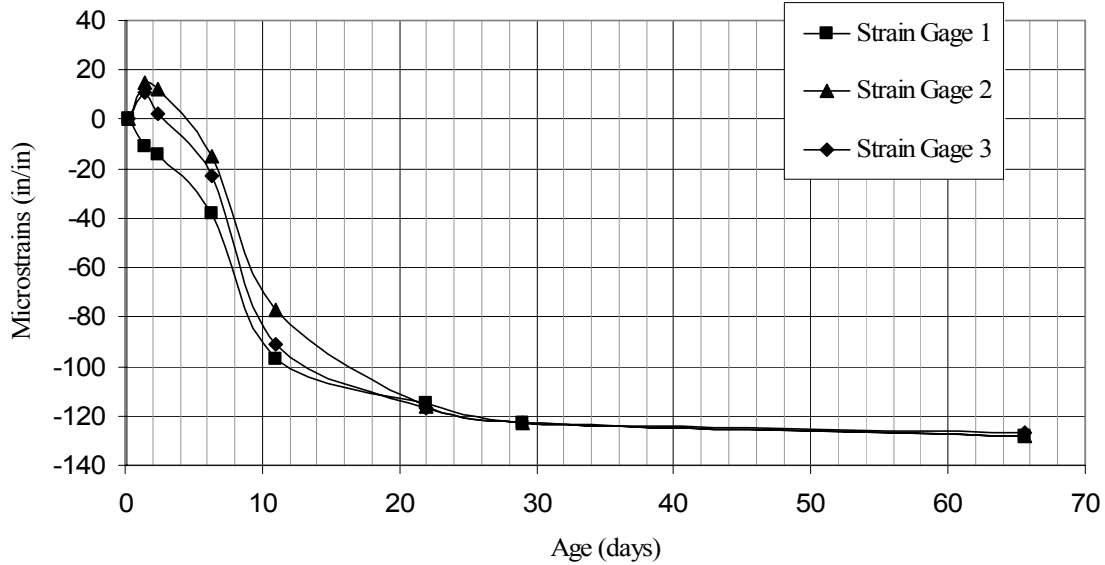


Figure 11. Shrinkage specimen axial strain over time.

## FINITE ELEMENT MODELING AND ANALYSIS

### BRIDGE MODEL

A finite element model was developed to replicate and confirm the results of the bridge measurements. Span 2 of Phase 2 was modeled using GTSTRUDL©, a general purpose frame and finite element analysis software program. The bridge deck was modeled using a finite element mesh of 1624 plate bending and stretching quadrilateral elements.

Space frame members were used to model the AASHTO bridge girders and diaphragms. To capture the true properties of the composite deck-girder section, the analytical girders were given a connection eccentricity to the nodes which were located at the mid-plane of the finite elements. Figure 12, below, depicts the girder element geometry.

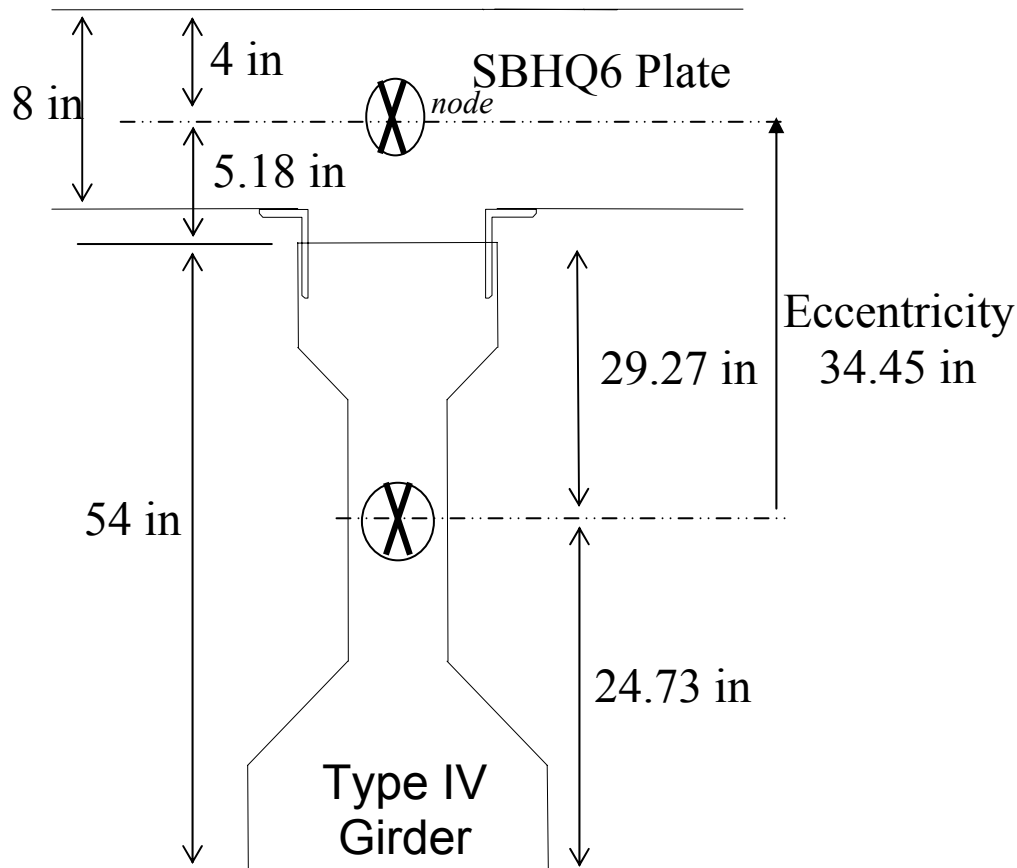


Figure 12. Eccentric connection, deck and girder analytical model.

Span 2 was modeled as a 124.1 ft (37.8 m) skewed simply-supported span. The boundary conditions for the model were initially idealized as a roller at the bent 2 support and a pin at the bent 3 support. A more realistic boundary condition was also modeled and considered. The roller bearing at the west support is a 2 inch (50 mm) elastomeric bearing, which was considered to provide some resistance to axial deformation. This model was used to assess the effect of the support restraint in the presence of a 50°F (28°C) uniform temperature change in the deck and girders. An average upward displacement of 0.007 inches (0.18 mm) resulted due to an incompatibility between the girder and deck coefficients of thermal expansion. The partial support restraint did not significantly affect the bridge deflection. Therefore, the idealized pin-roller support conditions were used for further computations.

## LOAD CASES

To model the bridge behavior and deflections, five load cases were developed. The results of the load cases were then superimposed to predict the total dead load deflection of the bridge.

The first load case considered was the self-weight of the bridge deck and was used for deflection predictions only. The second load case captured the thermal change in the deck from measured temperature of 76.6°F (24.8°C) at 4 hours after casting to the measured maximum heat of hydration of 107.8°F (42°C). The authors assumed that the bridge deck became composite with the girders 4 hours after casting. It was further assumed that the girders remained at the ambient air temperature while the deck heated and subsequently cooled. As the deck heated, the composite bridge girders were forced upward due to the deck's thermal expansion. The third load case modeled the thermal change in the deck from the measured maximum heat of hydration of 107.8°F (42 °C) to the ambient air temperature of 83°F (28°C). As the deck cooled, the composite bridge girders were forced downward due to the deck's thermal contraction.

The fourth load case considered was the barrier loading. The barrier load case modeled the dead load of the barrier located above Girder 2.13. The fifth load case modeled the unrestrained cooling of the entire bridge and was used for strain predictions only. The mechanical properties and loads for each of the load cases are outlined in Table 3 below.

The loading caused by shrinkage was not modeled. Laboratory tests indicated an average mid-plane contraction of -128 micro-strains. This shrinkage occurred in the presence of a 30°F (16.7°C) temperature change. Given an average CTE of 5.0  $\mu\epsilon/^\circ\text{F}$  (9  $\mu\epsilon/^\circ\text{C}$ ), the strain due to thermal effects was -150  $\mu\epsilon$ . The calculated thermal strain was very similar in magnitude to the observed laboratory strain, therefore thermal contraction was the primary mechanism for deck strain. Shrinkage of the deck was indistinguishable from thermal effects and not modeled as a separate load case.

Table 3. Five Load Cases and mechanical properties used for analysis.

Load Case	Description	Girder 56-day $E_c$	Deck $E_c$	$\Delta T$	Gravity Load
1	Deck Self-Weight	4,962 ksi (34,213 MPa)	—	0	4,700 lb/ft (6,994 kg/m)
2	Deck heating	4,962 ksi (34,213 MPa)	540 ksi (3.7 GPa)	31.1F 17 C	0
3	Deck cooling	4,962 ksi (34,213 MPa)	2,200 ksi (15.2 GPa)	24.8F 13 C	0
4	Barrier Load	4,962 ksi (34,213 MPa)	3,600 ksi (24.8 GPa)	0	437 lb/ft <sup>2</sup> (2,133 kg/m <sup>2</sup> )
5	Ambient Cooling	4,962 ksi (34,213 MPa)	3,600 ksi (24.8 GPa)	41.0F 23 C	0

#### ANALYTICAL MODEL OUTPUT

For each finite element analysis, the following data were reviewed: nodal displacement at 40% of the span length; mid-plane element strain and curvature; and girder member forces at 1/8 and 1/2 of the span length. The section modulus of the girders was used to calculate the strains at the top and bottom of the girders for each load case. The strain at the top and bottom of the concrete deck was calculated for each load case using the

mid-plane element strain and curvature. The analysis results are presented together with the field measurements.

**EXPERIMENTAL AND ANALYTICAL RESULTS**

**DISPLACEMENTS**

The experimental field measurements began with the placement of the concrete. The “zero” deflection condition of each girder was actually an average positive camber of 2.6 inches. Deflection measurements were then taken on Girders 2.9, 2.10, and 2.11 (north, center, and south pins shown in Figure 4).

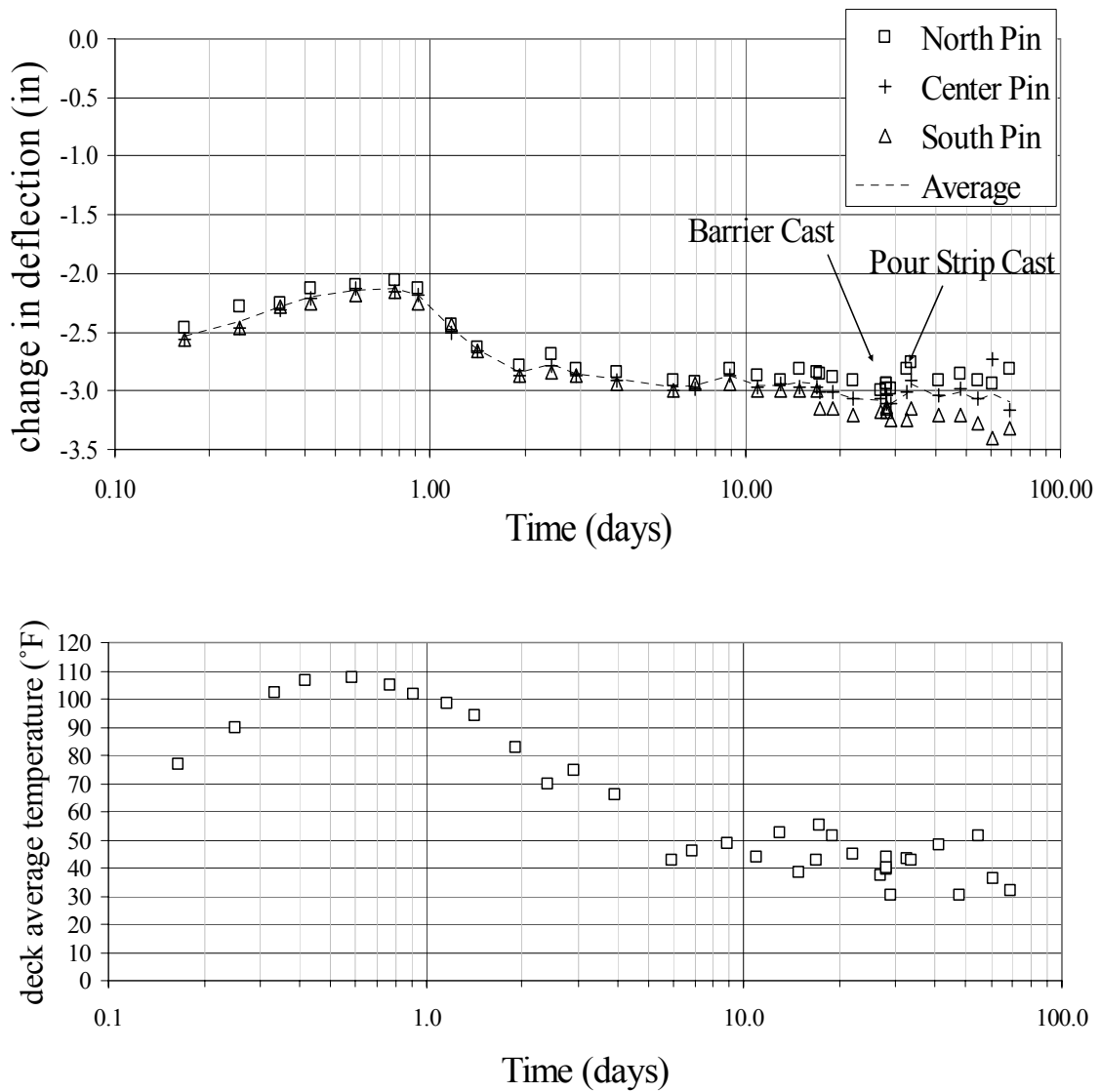


Figure 13. Midspan deflection (top) and ambient temperature (bottom).

Figure 13 plots the bridge deflection and associated temperatures in the concrete deck. In order to minimize temperatures differences between the deck and girder, measurements generally were taken before sunrise. Exceptions were at the time of concrete placement, day 0 when the deck was placed, and days 28 and 30 when the barrier was placed and the strip between Phases 1 and 2 was placed, respectively. The weight of the “wet” concrete induced an average downward deflection in the girders of 2.50 inches (64 mm) at the 0.4 L position. Table 4 shows the experimental and computed bridge deflection under the self-weight of the deck. The analysis over-predicted the displacement by less than 10%; a positive difference indicates that the analysis predicted greater deflection than measured.

Table 4. Experimental and analytical deck self-weight deflections.

Girder	Experimental	Analytical	Comparison	
	Deck Self-Wt	Deck Self-Wt	Difference	% Difference
North	-2.469 in (62.7 mm)	-2.6596 in (67.6 mm)	-0.191 in (-4.9 mm)	7.72%
Center	-2.563 in (65.1 mm)	-2.6635 in (67.7 mm)	-0.101 in (-2.6 mm)	3.92%
South	-2.563 in (65.1 mm)	-2.6491 in (67.3 mm)	-0.086 in (-2.2 mm)	3.36%

Figure 13 shows the deck concrete heating to a peak temperature of approximately 107.8 °F (42 °C) from an ambient temperature of 76.6 °F (24.8 °C). This heating induced an upward displacement of approximately 0.40 inches (10 mm) in the girders and was modeled in Load Case 2. Table 5 compares the experimental and analytical deflections caused by the deck heating. Analytical results were from -8 % to 5.8% of measured deflections.

Table 5. Experimental and analytical deck thermal expansion induced deflections.

Girder	Experimental	Analytical	Comparison	
	Thermal	Thermal	Difference	% Difference
North	0.375 in (9.5 mm)	0.388 in (9.9 mm)	0.013 in (0.33 mm)	3.52%
Center	0.438 in (11.1 mm)	0.403 in (10.2 mm)	-0.035 in (0.89 mm)	-8.06%
South	0.375 in (9.5 mm)	0.397 in (10.1 mm)	0.022 in (0.56 mm)	5.78%

An average deflection of approximately 0.89 inches (22.6 mm) occurred as the mean temperature in the deck dropped from its maximum of 107.8 °F (42 °C) to 83 °F (28 °C) (Load Case 3). Table 6 compares the experimental and analytical displacement of the bridge

caused by the cooling of the deck. The analysis under-predicted the actual deflection by an average of 32.7 %.

Table 6. Experimental and analytical deck thermal contraction induced deflections.

Girder	Experimental	Analytical	Comparison	
	Thermal	Thermal	Difference	% Difference
North	-0.833 in (-21.2 mm)	-0.6057 in (-15.4 mm)	0.277 in (7.0 mm)	-31.40%
Center	-0.977 in (-24.8 mm)	-0.6143 in (-15.6 mm)	0.363 in (9.2 mm)	-37.13%
South	-0.874 in (-22.2 mm)	-0.6102 in (-15.5 mm)	0.264 in (6.7 mm)	-30.18%

The change in deflection stabilized on day 2 at 83°F (28 °C). Deflections on days 3 through 6 were taken before sunrise when the temperature in the girders and deck were the same. At 28 days, the barrier was poured on the south side of the bridge. The self-weight of the barrier (load case 3) caused an additional average downward displacement of 0.09 inches. Table 7 compares the experimental and analytical displacements from the dead load of the barrier. The analysis under predicted the displacements between -114% and 37%, although the magnitude of the differences were less than 0.046 inches.

Table 7. Experimental and analytical barrier induced deflections.

Girder	Experimental	Analytical	Comparison	
	Barrier	Barrier	Difference	% Difference
North	0.031 in (0.8 mm)	-0.004 in (-0.1 mm)	-0.035 in (0.9 mm)	-114.2%
Center	-0.062 in (-1.6 mm)	-0.085 in (-2.2 mm)	-0.023 in (0.6 mm)	37.2%
South	-0.250 in (-6.4 mm)	-0.204 in (-5.2 mm)	0.046 in (1.2 mm)	-18.3%

Table 8 combines four of the five analytical load cases. Load case five did not cause a change in deflection and was used for strain calculations only. Table 9 lists the incremental and combined experimental results. Table 10 compares the total analytical deflections with experimental data. Combined analytical results underestimated total experimental deflections by less than 10%.

Table 8. Combined analytical deflections.

	DL	Expansion	Contraction	DL	
Girder	Deck Self-Wt	Thermal	Thermal	Barrier	Total
North	-2.6596 in (68.5 mm)	0.388 in (9.9 mm)	-0.6057 in (15.4 mm)	-0.0044 in (0.1 mm)	-2.8815 in (73.2 mm)
Center	-2.6635 in (67.7 mm)	0.403 in (10.2 mm)	-0.6143 in (15.6 mm)	-0.0851 in (2.2 mm)	-2.9601 in (75.2 mm)
South	-2.6491 in (67.3 mm)	0.397 in (10.1 mm)	-0.6102 in (15.5 mm)	-0.2043 in (5.2 mm)	-3.0670 in (77.9 mm)

Table 9. Experimental deflections.

	DL	Expansion	Contraction	DL	
Girder	Deck Self-Wt	Thermal	Thermal	Barrier	Total
North	-2.469 in (-62.7 mm)	0.375 in (9.5 mm)	-0.883 in (-22.4 mm)	0.0310 in (-0.8 mm)	-2.946 in (-75 mm)
Center	-2.563 in (-65.1 mm)	0.438 in (11.2 mm)	-0.977 in (-24.8 mm)	-0.0620 in (-1.6 mm)	-3.164 in (-80 mm)
South	-2.563 in (-65.1 mm)	0.375 in (9.5 mm)	-0.874 in (-22.2 mm)	-0.2500 in (-6.4 mm)	-3.312 in (-84 mm)

Table 10. Comparison of experimental and analytical results.

Girder	Experimental	Analytical	Difference	Difference
North	-2.946 in (-74.8 mm)	-2.882 in (-73.2 mm)	-0.065 in (-1.8 mm)	-2.19%
Center	-3.164 in (-80.4 mm)	-2.960 in (-75.2 mm)	0.204 in (3.9 mm)	-6.44%
South	-3.312 in (-84.1 mm)	-3.067 in (-77.9 mm)	0.245 in (4.0 mm)	-7.40%

## STRAIN

Strain gages within the bridge deck and bonded to the tops of girders measured strain over time. Figures 14 and 15 give the measured electrical resistance strain gage data at midspan and 1/8-span locations for Girder 2.10. Figures 16 and 17 give the measured vibrating wire and electrical resistance strain gage data for Girder 2.9 at midspan. The two strain gages for Girder 2.9 provided conflicting profiles for strain in the deck. The electrical resistance strain gage registered a 400 microstrain tensile strain near the top of the deck, where a compressive strain would be expected. The largest magnitude tensile strain recorded

by the vibrating wire gage was 64 microstrains. Comparing the vibrating wire data to the temperature plot in Figure 13, the deck appears to compress during heating and expand during cooling. However, the vibrating wire data at 70 days appears to make sense and was used for further analysis. For all strain plots, positive strain indicates elongation. The zero point for all measurements occurred at 4 hours after the casting of the deck. Therefore, the self-weight of the deck was not considered in strain measurements or analytical predictions.

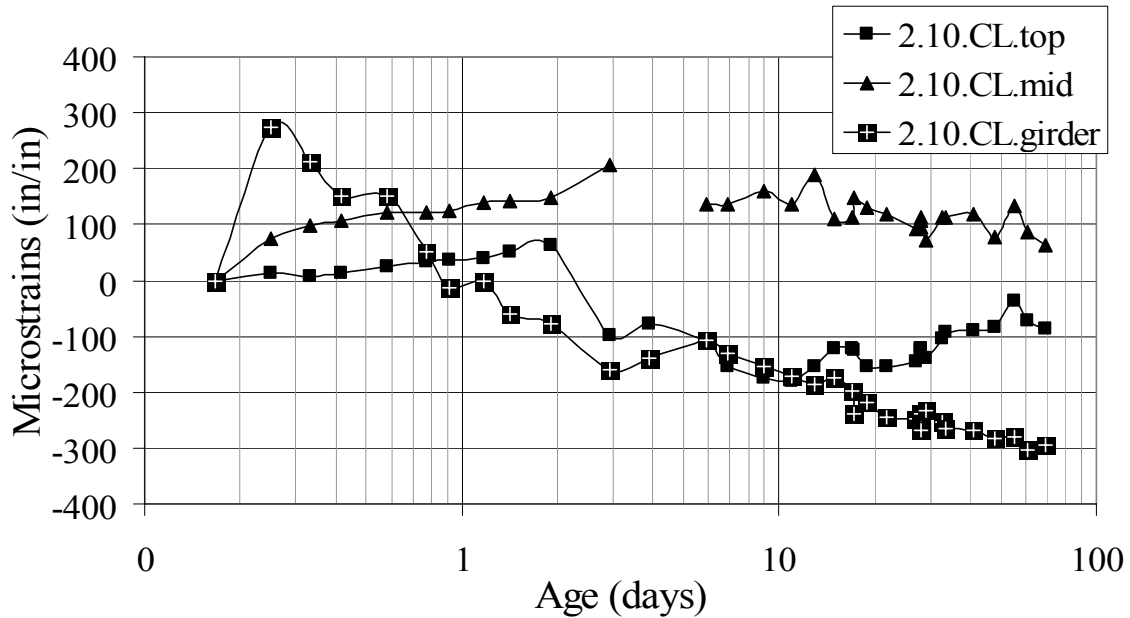


Figure 14. Strain profile (corrected for temperature) at midspan, Girder 2.10.

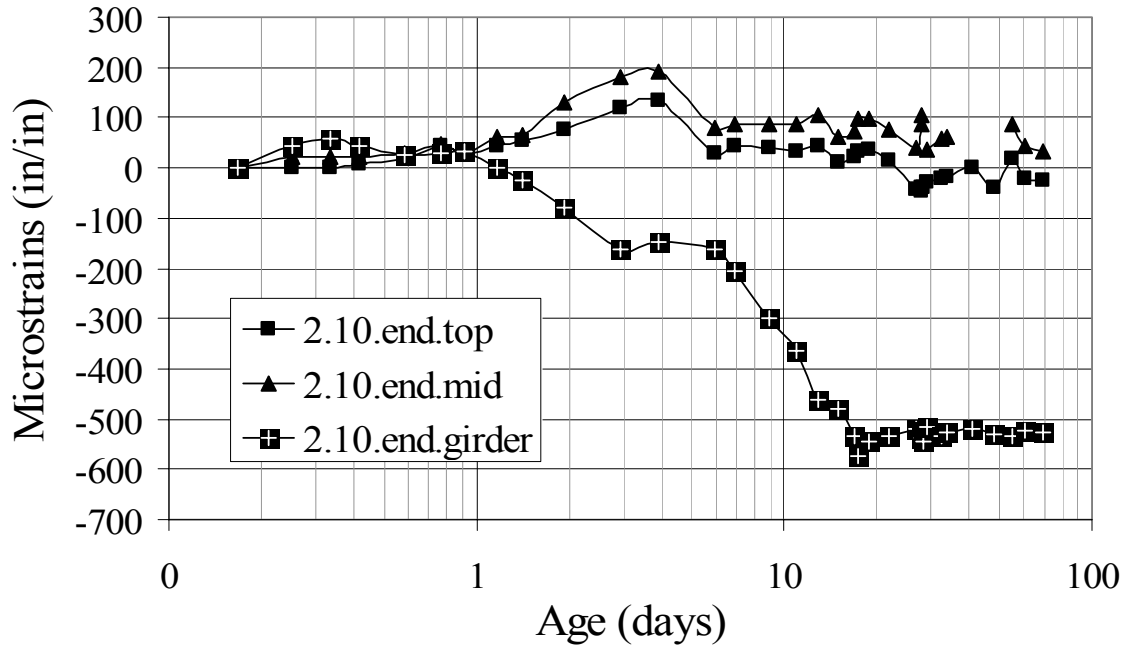


Figure 15. Strain profile at end, 1/8 – span, Girder 2.10.

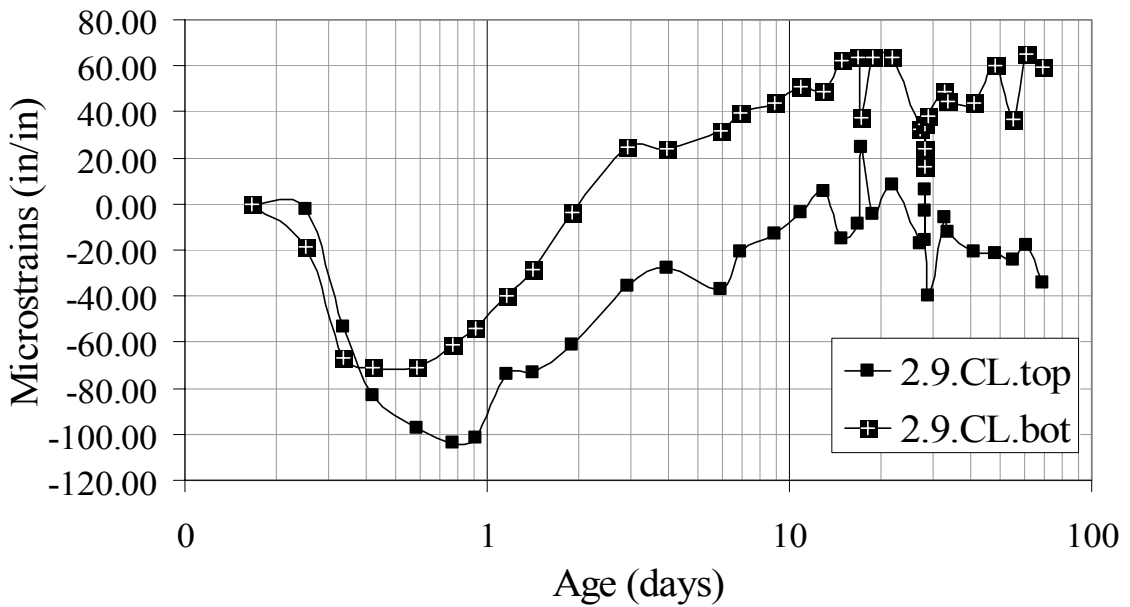


Figure 16. Vibrating wire strain data at midspan, Girder 2.9.

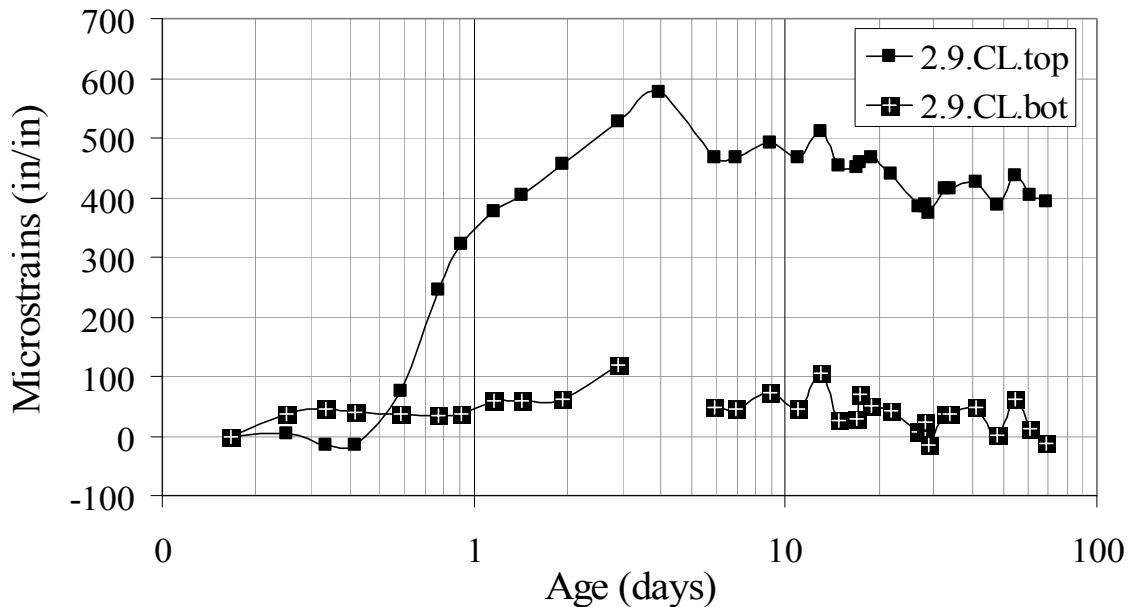


Figure 17. Electrical resistance strain data at midspan, Girder 2.9

Load cases 2 through 5 were combined to produce the analytical strain profiles in the bridge deck and girders. Strain data from the analytical model are presented in Table 11 for each load case at the 1/8 – span and midspan locations. Figures 18 and 19 compare the experimental and analytical strain results at midspan at 70 days. Figures 20 and 21 compare the experimental and analytical strain results at the 1/8 – span location at 70 days. The electrical resistance strain gage for Girder 2.10 at the 1/8 L location showed an unexplained 300 microstrain increase in compression from day 7 to day 17. This jump in strain was not associated with any change in loading or significant temperature change. Figure 20 presents the strain profile as recorded, while Figure 21 provides a corrected strain profile for comparison. The analytical strain at the top of the girders closely matches the experimental strain data for each of the measured locations. The strain in the deck, however, was different from measured strain data. Strain measurements in the bridge deck show significantly larger curvatures and approximately 100 microstrains less compression at the midplane than analytical predictions.

Table 11. Analytical strain data.

Load Case	Location	E (ksi)	Midspan	1/8 L
			Strain (microstrains)	Strain (microstrains)
Deck Heating	Deck Top	540	210	206
Deck Heating	Deck Bottom	540	198	194
Deck Heating	Girder Top	4962	44	40
Deck Heating	Girder Bottom	4962	-38	-34
Deck Cooling	Deck Top	2200	-107	-107
Deck Cooling	Deck Bottom	2200	-89	-88
Deck Cooling	Girder Top	4962	-69	-67
Deck Cooling	Girder Bottom	4962	58	57
Barrier	Deck Top	3600	-14	-10
Barrier	Deck Bottom	3600	-11	-9
Barrier	Girder Top	4962	-12	-7
Barrier	Girder Bottom	4962	10	6
Ambient Cooling	Deck Top	3600	-204	-203
Ambient Cooling	Deck Bottom	3600	-204	-203
Ambient Cooling	Girder Top	4962	-212	-212
Ambient Cooling	Girder Bottom	4962	-212	-212
Summation	Deck Top	Combined	-116	-114
Summation	Deck Bottom	Combined	-106	-106
Summation	Girder Top	Combined	-249	-247
Summation	Girder Bottom	Combined	-181	-183

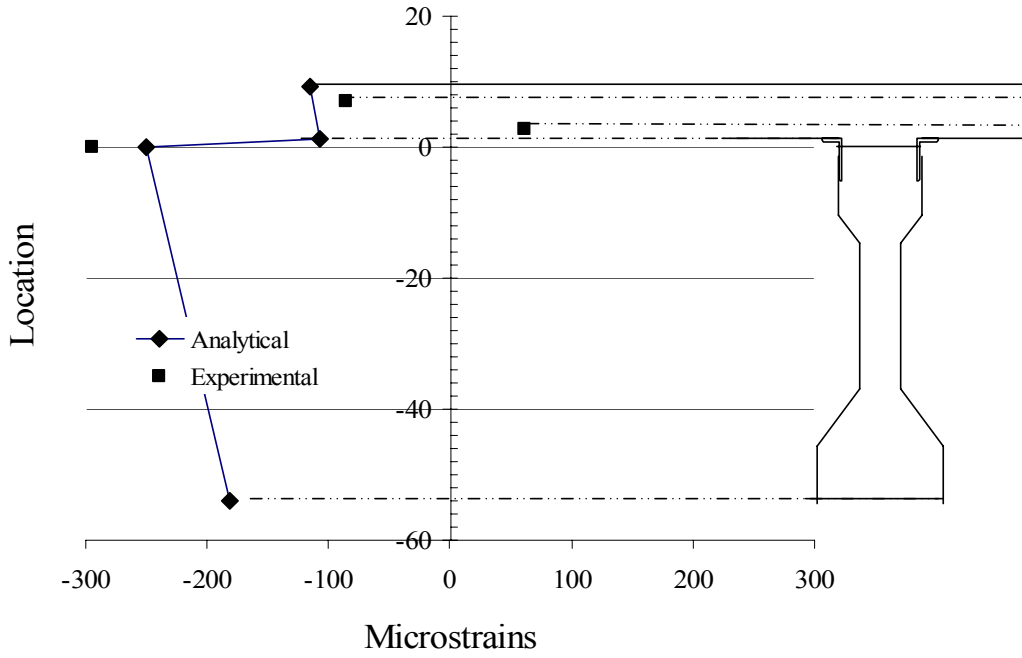


Figure 18. Experimental and analytical strain profile at midspan, Girder 2.10, at 70 days.

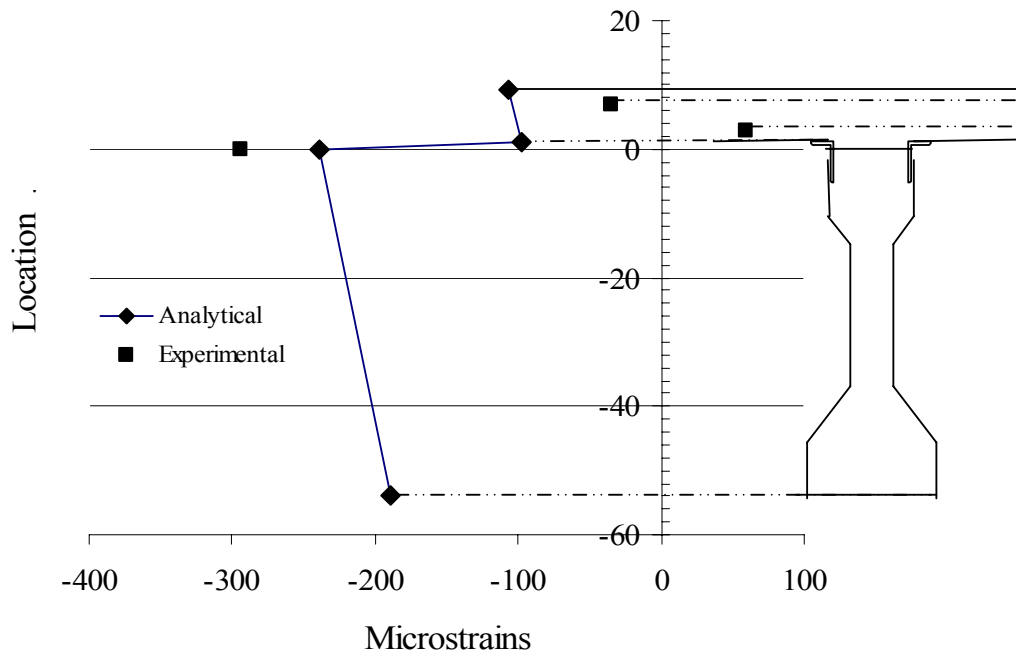


Figure 19. Experimental and analytical strain profile at midspan, Girder 2.9, at 70 days.

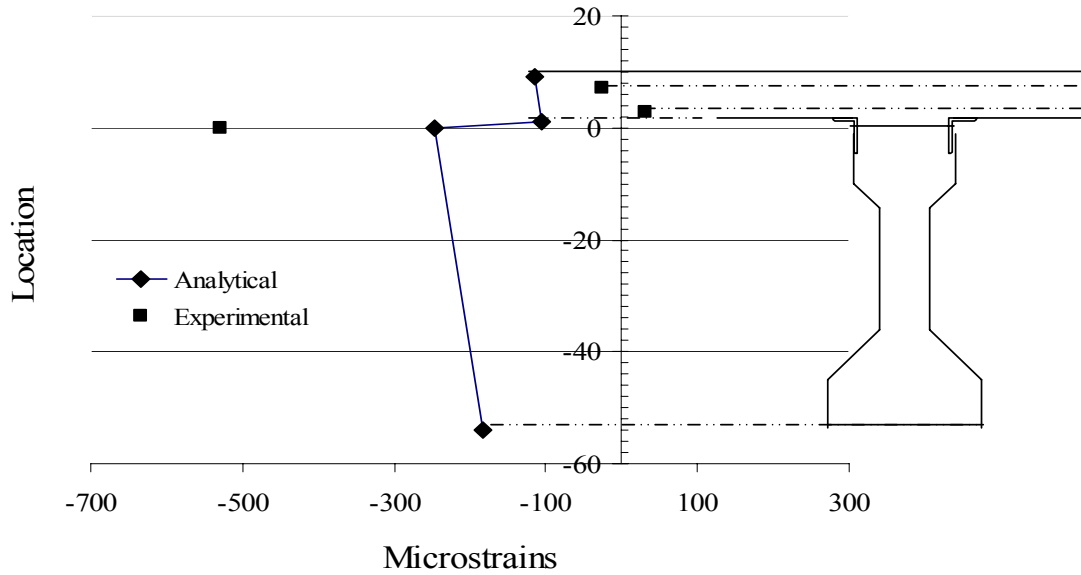


Figure 20. Uncorrected experimental and analytical strain profile at 1/8 – span, Girder 2.10, at 70 days.

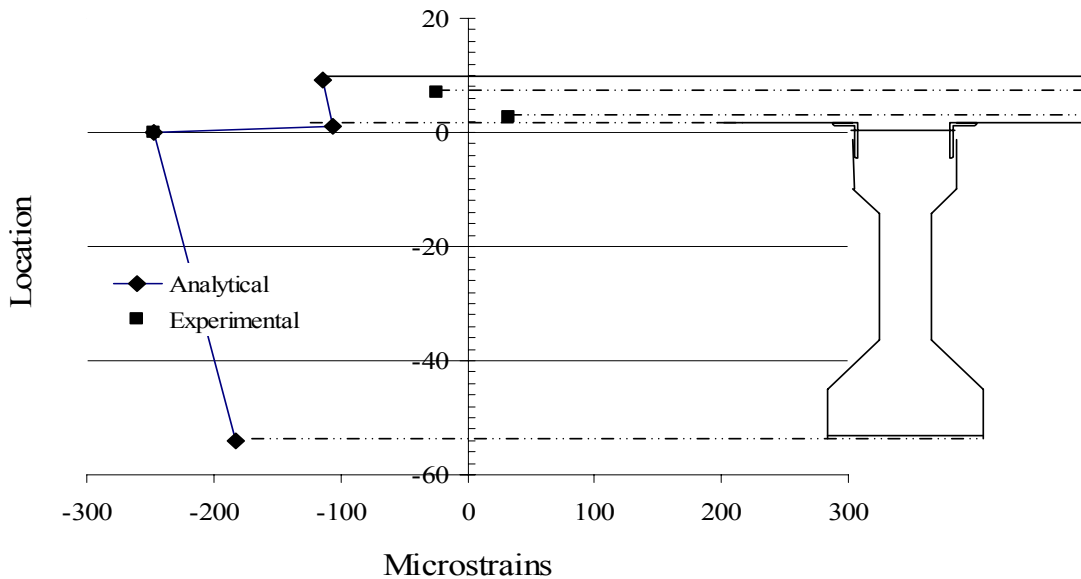


Figure 21. Corrected experimental and analytical strain profile at 1/8 – span, Girder 2.10, at 70 days.

## DISCUSSION

### DEFLECTION

The analytical model was developed to confirm the causes of the experimental deflections for Phase 2 of the high performance bridge project. As noted before, a downward deflection of 1.3 inches (33 mm) was observed in Phase 1 of the project. According to Slapkus and Kahn (2002), the initial measured camber for the Type IV girders in span 2 for Phases 1 and 2 was approximately 2.5 inches (64 mm). Superimposing the deck self-weight deflection of approximately 2.5 inches (64 mm) would result in a flat bridge with 0 inches of deflection. Therefore, the additional 1.3 inches (33 mm) of deflection was unexplained. According to experimental data in Phase 2, span 2 displaced an average of 3.1 in (78.7 mm) downward, with 0.54 in (13.7 mm) of downward deflection occurring after the application of the deck and barrier self-weights.

Standard design models assume there are no additional dead load deflections past the application of the deck and barrier self-weights. Two theories were suggested to explain the additional deflection – slipping (non-composite behavior) between the deck and girders or deck contraction. The first question to be answered was whether the girders and deck were acting as a composite member. The initial heating and expansion of the deck (Load Case 2) caused an apparent average upward deflection of approximately 0.40 in (10.2 mm) at 40% L. Next, the cooling and contraction of the deck (Load Case 3) caused an apparent average downward deflection of 0.89 inches (22.6 mm) at 40% L. Assuming fully composite action, analytical results yielded an initial upward average deflection of 0.40 in (10.2 mm) followed by a downward average deflection of 0.61 inches (15.5 mm). These analytical results at the north, center, and south pins varied from -37.1 % to 5.8 % of the experimental data. The correlation in analytical and experimental results for these two load cases suggests that the girders and deck were generally acting as a fully composite section. The higher deflections in the field measurements are believed to result from autogenous shrinkage (approximately 32% of thermal contraction) in the deck. The shrinkage occurred simultaneous to the thermal contractions, causing deflections that were not captured analytically.

The self-weight of the barrier (Load Case 4) was applied to analytical models of the bridge using both fully composite behavior and non-composite behavior. The results of the two analyses established upper and lower bounds for composite action in the bridge and were compared with experimental data in Table 12. The measured maximum deflection of -0.25 inches occurred at the south pin, closest to the barrier. The analytical upper and lower bounds for deflection at the north pin were -0.2043 inches and -0.4779 inches, respectively. The experimental results were within 25% of the fully composite (upper bound) analysis. This result confirmed that the bridge deck and girder were generally acting as a composite section.

Table 12. Comparison of composite and non-composite bridge deflection due to barrier self-weight (Load Case 4).

	Analytical	Experimental	Analytical
Girder	Composite		Non-Composite
North	-0.0044 in (-0.1 mm)	0.031 in (0.8 mm)	-0.0580 in (-1.5 mm)
Center	-0.0851 in (-2.2 mm)	-0.062 in (-1.6 mm)	-0.2244 in (-5.7 mm)
South	-0.2043 in (-5.2 mm)	-0.250 in (-6.4 mm)	-0.4779 in (-12.1 mm)

The dead load of the concrete barrier also influenced the behavior of the bridge. The barrier was cast in place and positively connected to the bridge deck. Experimental results from Phase 2 revealed additional deflections of 0.03 (0.8 mm) and -0.25 inches (6.4 mm) at Girder 2.9 (north) and Girder 2.10 (south), respectively. The south girder was closest to the barrier and experienced the larger deflection. Analytical results suggested downward displacements of 0.004 (0.1 mm) and 0.204 inches (5.2 mm), respectively. The analytical results differed by -114% to -37% from the experimental data, with differences less than 0.05 inches. These results confirm that the barrier's dead load can affect the deflection of the bridge.

The finite element analysis produced total girder deflections within -2.2 % to -7.4% of experimental results. The close correlation between the analytical results and experimental data confirm the cause of the unexpected bridge deflections. Experimental results for span 2 during Phase 2 of the project revealed additional girder deflections of 0.50 (12.7 mm) to 0.54 inches (13.7 mm) after the application of the deck and barrier self-weights. The additional deflections were primarily a result of thermal contractions in the bridge deck. The concrete achieved heats of hydration in excess of 100°F (38°C) during the curing process. Since the concrete for the deck was cast during the month of November, the temperature of the fresh concrete was 40°F (22°C) to 60°F (33°C) higher than ambient temperatures. The hot, newly cast concrete locked onto the girders and began to contract. The differential contraction thus caused the additional deflections.

Analytical results for midspan deflection were 6.44% less than experimental data. The authors believe this difference was due to shrinkage in the bridge deck. Shrinkage samples of deck concrete were unable to separate the effects of shrinkage from thermal actions. The un-modeled shrinkage of the deck concrete was the likely cause of the differences in experimental and analytical results.

The observed additional deflection in Phase 1 was 1.3 inches (33 mm), approximately 0.5 inches (13 mm) greater than Phase 2. The authors believe the cause of the deflection is the same. However, the conditions surrounding the construction of Phase 1 were somewhat different. Factors that may have influenced the deflections in Phase 1 include differences in coefficients of thermal expansion, ambient temperature conditions during the deck pour, and mechanical properties of the deck concrete. Further, the girders for both phases were cast at

the same time. The girders for Phase 2 were loaded at 425 days, while the Phase 1 girders were loaded at 60 days. The age of the girders at the time of construction may also have affected the deflections of the two phases differently.

Span 2 (124 ft, 37.8 m) of the high performance bridge represented the longest span Type IV girder bridge in the State of Georgia. The phenomena of deck contraction induced deflections also could be present in other bridges, but may not have been noticed. Similar Type IV AASHTO bridges in the state have lengths of about 90 ft (27.4 m). An analysis was conducted on a 90-ft span to compare deflection results. All other variables remained constant in the model. Table 13 below suggests that deflections in normal span bridges (90 ft, 27.4 m) are 38% of those predicted for a long span bridge (124 ft, 37.8 m).

Table 13. Comparison of deflections by span length.

Span Length	Dead Load Deck Self-Wt	Deck Thermal Contraction	Dead Load Barrier	Total
124 feet (37.8 m)	-2.6635 in (-67.7 mm)	-0.6143 in (-15.6 mm)	-0.0851 in (-2.2 mm)	-2.960 in (-75.2 mm)
90 feet (27.4 m)	-0.7750 in (-19.7 mm)	-0.3313 in (-8.4 mm)	-0.0196 in (-0.5 mm)	-1.126 in (-28.6 mm)
Difference	1.8885 in (48.0 mm)	0.2830 in (7.2 mm)	0.0654 in (1.7 mm)	1.834 in (46.6 mm)
% Difference	-244%	-85%	-333%	-163%

## STRAIN

Measured strain profiles in span 2 of Phase 2 show compression at the top of the deck concrete and at the top of the girders. The compressive strain in the deck was caused by the thermal contraction from the peak heat of hydration to ambient conditions. The deck is restrained from thermal shrinkage and contraction by its connection to the girders; thus tensile stresses are induced as the concrete contracts. As the contraction occurs in the deck concrete, a compressive strain is induced at the top of the girder.

The analytical strain profiles at midspan and 1/8 L match the measured strain at the top of the deck and the top of the girders. Analytical predictions for strain at the bottom of the deck differ significantly from measured data. The measured profile in the deck shows compressive strain at the top and tensile strain at the bottom, whereas the analytical model predicts compression at both the top and bottom. Analytical strains in the deck were an average of 100 microstrains greater in compression. One exception to the mismatch in deck strains was the analytical result at the top of the deck—it appears to lie in a straight line with the measured strain data within the concrete deck in Figures 18, 19, and 21. The significant difference between analytical and experimental results appears to be in the strain at the bottom of the deck.

Analytical predictions for strain at the top of the girders were within  $\pm 50$  microstrains of measured girder strains. The analytical results are similar for each of the

locations at midspan and at  $1/8 L$ . The closely matching girder strains suggest that the girders and deck were acting as a fully composite section, while the large curvature shown by deck strains indicate possible non-composite behavior. The analytical model assumed perfect compatibility at the interface between the deck and girders. The measured strains and large curvatures, however, indicated that full compatibility was not present. The lack of compatibility at the interface would have caused less restraint to axial deformation and significant flexure in the deck.

A large change in curvature in the concrete deck appeared to occur between days 1 and 3. Figures 22, 23, and 24 plot the experimental strain profiles at 1, 3, and 7 days, respectively, relative to the 70 day analytical strain profile for Girder 2.10 at midspan. The large change in curvature in the concrete deck occurred between days 1 and 3, and did not change between days 3 and 7. This data suggests that the curvature in the concrete deck occurred during the first 3 days, before the concrete gained significant strength. The large curvature was “locked in” to the bridge deck allowing only small changes in curvature as the bridge aged. Drying at the exposed top surface of the deck caused a large amount of shrinkage due to water loss. The bottom surface of the concrete, however, was protected by the metal deck and appeared to shrink less. The difference in conditions at the top and bottom surfaces of the bridge deck may have caused differential drying and induced a large curvature between days 1 and 3.

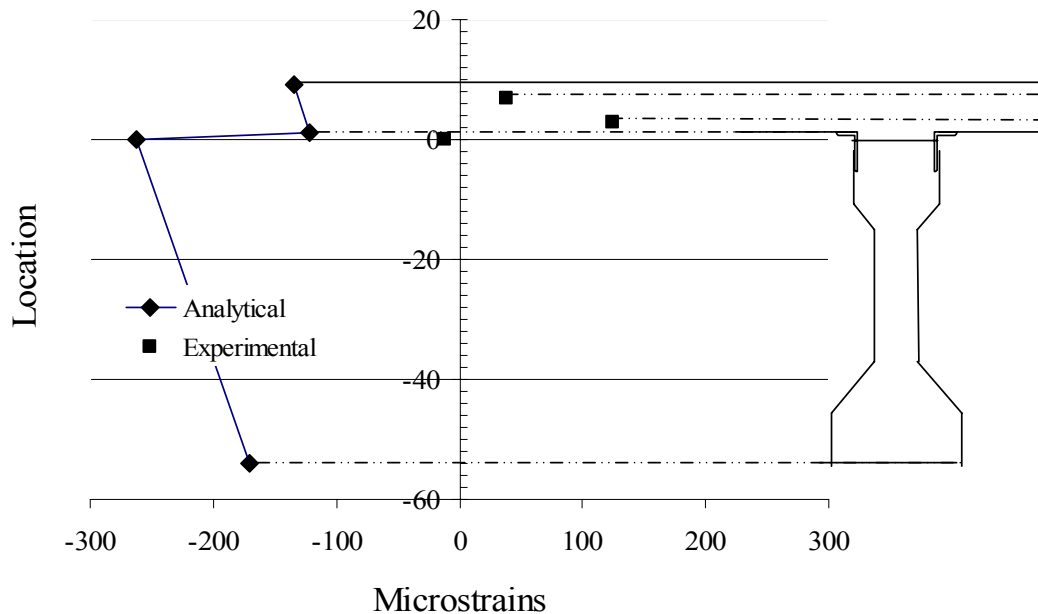


Figure 22. Experimental strain profile, midspan, Girder 2.10, at 1 day, compared to 70 day analytical strain.

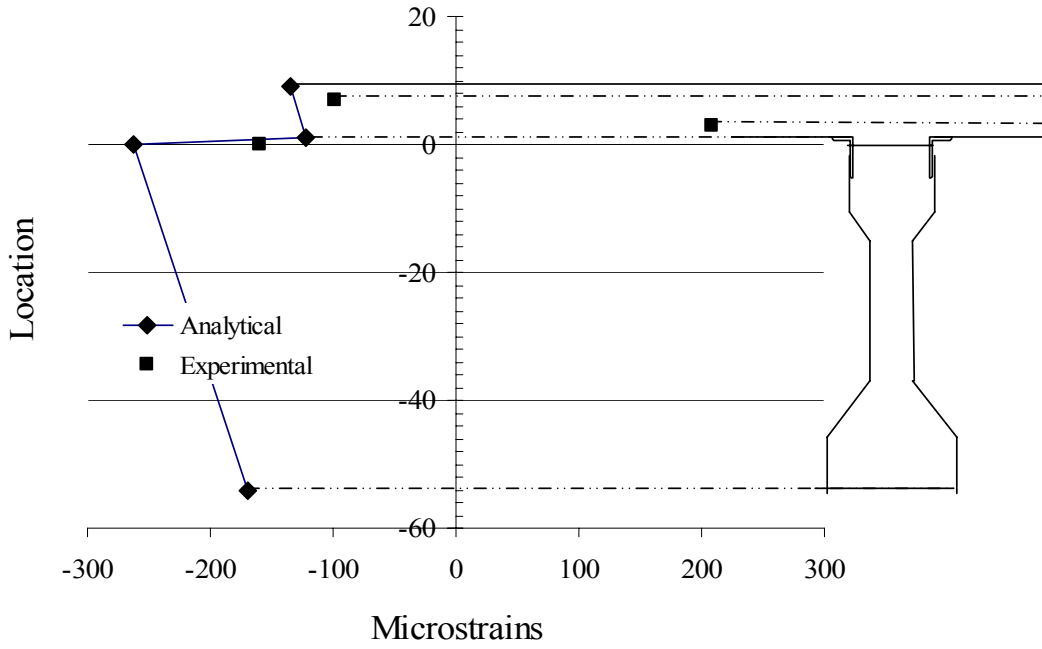


Figure 23. Strain profile, midspan, Girder 2.10, at 3 day, compared to 70 day analytical strain.

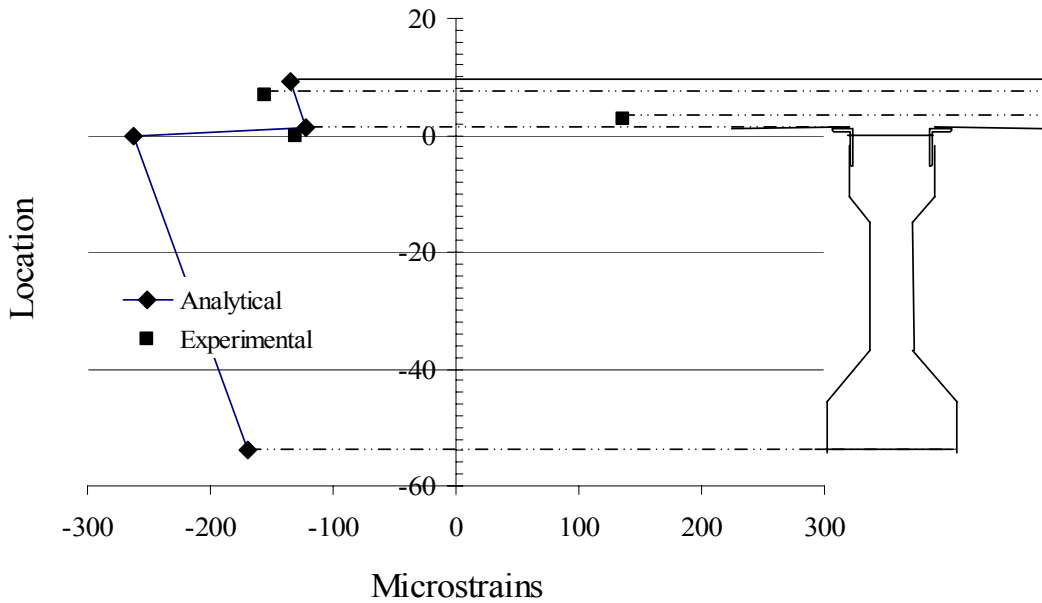


Figure 24. Strain profile, midspan, Girder 2.10, at 7 days, compared to 70 day analytical strain.

Figures 14 and 15 depict a slight, steady increase in compressive strain in the deck from 3 days after casting to 70 days. The ambient temperature dropped 41°F during this period. The same figures depict a steeper increase in compressive strain at the top of the girders. The girders appear to be contracting more as the ambient temperature drops, as modeled in Load Case 5. The difference in behavior could be explained by a difference in the strain gages. The strain gages for the girders are bonded to the top of the girders and covered with silicone to prevent bonding to the deck. The strain gages for the deck, however, were embedded in the concrete next to continuous steel reinforcement. The continuity of steel reinforcement in the concrete deck provided partial restraint to axial deformations and was not modeled analytically. The attached strain gage at the top of the girder would have indicated more deformation due to ambient temperature changes. Another source of difference was the epoxy coated deck reinforcement at the top and un-coated reinforcement at the bottom of the deck. The difference in bonding behavior between the two types of reinforcement may have led to the large curvature in deck strain profiles.

The analytical and experimental results for strain confirm that shrinkage and temperature strains occurred in the bridge deck and induced compression at the top of the girders. These compressive strains caused significant deflections in span 2, beyond those induced by dead loads. The lack of correlation between analytical and experimental deck strain leads to several unanswered questions. The differences in strain magnitude and curvature suggest uncertainty in the amount of restraint provided by deck reinforcement, the differences in embedded and attached strain gage behavior, the validity of this model in predicting strain, and the amount of compatibility between the deck and girders.

## DESIGN CONSIDERATIONS

Contraction of the deck concrete during the curing cycle was the primary cause for the excess deflection in the Phase 2 span. To account for the added deflection due to thermal changes in the deck, a simplified approach has been developed. Assuming a constant state of strain in the deck due to thermal changes, an equivalent axial force can be calculated using a stiffness relationship.

$$F_e = k \cdot \Delta_T \quad (1)$$

$$\text{where } \Delta_T = \alpha_{\text{deck}} \cdot \Delta T \cdot L_{\text{span}} \quad (2)$$

$$k = E_{\text{deck}} \cdot A / L_{\text{span}} \quad (3)$$

$$A = b_{\text{eff}} \cdot h_f \quad (4)$$

The equivalent axial force, acting through the midplane of the deck and at an eccentricity from center of the transformed composite section, causes an equivalent uniform moment.

$$M_e = F_e \cdot e \quad (5)$$

$$\text{where } e = y_t' - h_f / 2 \quad (6)$$

Finally, an estimated midspan, maximum deflection can be predicted by the equation for a simply supported beam with constant end moments. Note that the moment of inertia ( $I_T$ ) of the girder-deck transformed section is calculated using an approximation for the 2 day modulus of elasticity for the deck concrete ( $E_{\text{deck},i} \approx 60\% E_{\text{deck}}$ ).

$$\Delta = M_e \cdot L_{\text{span}}^2 / (E_{\text{girder}} \cdot I_T) \quad (7)$$

In the case of span 2, Phase 2, the maximum midspan deflection due to the contraction of the deck was 0.54 inches (13.7 mm) after the application of the dead load. Equation 7 predicts a deflection of 0.606 inches (15.4 mm) for span 2, Phase 2. Given the data from this limited study, the equations above provide a simple and apparently conservative estimate for the deflections induced by deck contraction.

## CONCLUSIONS AND RECOMMENDATIONS

### CONCLUSIONS

Phases 1 and 2 of the high performance bridge project exhibited larger dead load deflections than predicted by design calculations. Phase 2 of the project was instrumented and evaluated in order to determine the cause of the added deflections. Experimental data and analytical results suggest that thermal contraction of the deck was the primary cause of the additional displacement. Additional downward displacements were also caused by shrinkage contractions in the deck, although these effects were relatively small compared to thermal contractions. Analytical predictions of total bridge displacements were within 10% of the experimental data. Further, the measured strain profiles in the girders matched those provided from analysis. Strain profiles in the bridge deck, however, differed significantly from analytical predictions.

### RECOMMENDATIONS

For bridges made with high strength concretes when the span lengths are significantly greater than previously used for the same depth girder, the effects of deck contraction should be considered during design. Equation 7 provides a simplified method for predicting the induced girder deflection due to deck contraction. Additional research should be conducted to further study and understand the effects of deck contraction on bridge behavior. Additional research is needed to determine the autogenous shrinkage of high performance concrete decks and its effect on deflection. More study is needed to verify the assumption of composite behavior and to determine the point during the curing cycle when composite behavior is achieved. Limited studies of shrinkage samples suggest that the coefficient of thermal expansion for high performance concrete can vary greatly with age. Further investigation is needed to fully understand the CTE of high performance concrete. Finally, deck and girder composite sections should be examined in future studies to determine the cause of the deck strains observed in this study.

## ACKNOWLEDGEMENTS

This research was sponsored by the Georgia Department of Transportation under Georgia Department of Transportation Research Project No. 9510.

The contents expressed herein reflect the views of the authors who are responsible for the facts and the accuracy of the data presented. The contents do not necessarily reflect the official views or policies of the Federal Highway Administration or of the Georgia Department of Transportation. This paper does not constitute a standard, specification, or regulation.

## REFERENCES

1. Slapkus, A. and Kahn, L., "Evaluation of Georgia's High Performance Concrete Bridge," Structural Engineering, Mechanics and Materials, Research Report No. 03-3, Georgia Institute of Technology, Atlanta, GA, 2002.
2. CRD-C39. "Test Method for Coefficient of Linear Thermal Expansion of Concrete," U.S. Army Corps of Engineers, Handbook for Concrete and Cement, June 1981, pp. 1-2.

## APPENDIX A – NOTATION

$A$	=	Area of deck contributing to composite girder/deck section, in <sup>2</sup>
$\alpha_{\text{deck}}$	=	Deck concrete coefficient of thermal expansion, in/in/°F
$b_{\text{eff}}$	=	Effective width of concrete deck, contributing to 1 girder, in
$\Delta$	=	Total vertical bridge deflection at midspan due to deck contraction, in
$\Delta_T$	=	Axial deformation in the bridge deck, in
$\Delta T$	=	Change in temperature due to curing in the bridge deck concrete from the peak heat of hydration to ambient, °F
$e$	=	Eccentricity of deck axial force, with respect to transformed section center of gravity, in
$E_{\text{girder}}$	=	Modulus of elasticity of girders, ksi
$E_{\text{deck},i}$	=	Modulus of elasticity of deck at 2 days used to calculate transformed early age section properties, ksi
$F_e$	=	Equivalent axial force in concrete deck due to thermal contraction, kips
$h_f$	=	Height or thickness of deck concrete, in
$I_T$	=	Moment of inertia of transformed deck-girder section, in <sup>4</sup>
$k$	=	Axial stiffness of bridge deck, kip/in
$L_{\text{span}}$	=	Length of span of girder, in
$M_e$	=	Equivalent end moment due to thermal deck contraction, in-kips
$y_t'$	=	Distance from center of gravity of deck-girder transformed section to top of deck, in